arXiv:0901.1750v2 [hep-ph] 16 Apr 2009

ULB-TH/09-02

Neutrinos from Inert Doublet Dark Matter

Sarah Andreas[†,‡], Michel H.G. Tytgat[†] and Quentin Swillens[†,⋆]

[†] *Service de Physique Théorique, Université Libre de Bruxelles, CP225, Bld du Triomphe, B-1050 Brussels, Belgium*

[‡] *Institut für Theoretische Physik E RWTH Aachen University, D-52056 Aachen, Germany*

[⋆] *IIHE-Inter-University Institute for High Energies, Université Libre de Bruxelles, B-1050 Brussels, Belgium*

Sarah.Andreas@rwth-aachen.de; mtytgat@ulb.ac.be; qswillen@ulb.ac.be

Abstract

We investigate the signatures of neutrinos produced in the annihilation of WIMP dark matter in the Earth, the Sun and at the Galactic centre within the framework of the Inert Doublet Model and extensions. We consider a dark matter candidate, that we take to be one of the neutral components of an extra Higgs doublet, in three distinct mass ranges, which have all been shown previously to be consistent with both WMAP abundance and direct detection experiments exclusion limits. Specifically, we consider a light WIMP with mass between 4 and 8 GeV (low), a WIMP with mass around 60-70 GeV (middle) and a heavy WIMP with mass above 500 GeV (high). In the first case, we show that capture in the Sun may be constrained using Super-Kamiokande data. In the last two cases, we argue that indirect detection through neutrinos is challenging but not altogether excluded. For middle masses, we try to make the most benefit of the proximity of the so-called 'iron resonance' that might enhance the capture of the dark matter candidate by the Earth. The signal from the Earth is further enhanced if light right-handed Majorana neutrinos are introduced, in which case the scalar dark matter candidate may annihilate into pairs of mono-energetic neutrinos. In the case of high masses, detection of neutrinos from the Galactic centre might be possible, provided the dark matter abundance is substantially boosted.

1 Introduction

Cosmological observations concur to indicate that about 25 % of the energy density of the universe is made of dark matter (DM) [1, 2]. The simplest and most popular paradigm postulates that dark matter is a weakly interacting massive particle or WIMP [3, 4]. The reason is twofold. Firstly, a stable particle with annihilation cross section in the picobarn range, characteristic of weak interactions, would have a relic density in agreement with observations, $\Omega_{DM} \propto 1/\langle\sigma v\rangle \sim 0.25$. Secondly, supersymmetric extensions of the Standard Model predict the existence of a dark matter candidate which, generically, is a spin 1/2 particle with weak scale interactions, the neutralino. There is also a popular spin 1 WIMP candidate, in the form of the lightest Kaluza-Klein partner of the photon in models with Universal Extra Dimensions (UED) [5]. To complete the list, one may consider the Inert Doublet Model (IDM), a very simple extension of the Standard Model introduced in ref. [6]. This model has two Higgs doublets and, to prevent FCNC, a discrete Z_2 symmetry. The dark

matter candidate is the lighest neutral component of the extra Higgs doublet.[1] Clearly, it is not the ambition of the IDM to compete with, say, the MSSM or UED models. This model is however very simple and, nevertheless, it does have interesting phenomenological consequences, some of which have been emphasized in recent works, refs. [8, 9, 10]. Furthermore, its dark matter features are not less interesting, both from the perspective of direct detection and indirect detection, be it through gamma rays [11, 12], neutrinos [13], or antimatter [14].

To complete the analysis of IDM dark matter phenomenology initiated in refs. [8, 9, 10, 11, 12, 13, 14, 15, 16], we discuss further the signatures of the IDM dark matter candidate in neutrinos.[2] Specifically, we consider three distinct dark matter mass ranges which we call in the sequel, the low, middle and high mass ranges. All are consistent with WMAP abundance and we consider the potential for indirect detection of these IDM dark matter candidates through the flux of neutrinos that might be produced in its annihilation in the Sun (low mass range), in the Earth (middle mass range), or at the Galactic centre (GC) (high mass range).

As discussed in ref. [16], the IDM dark matter candidate may be rather light, $m_{DM} \sim$ few GeV (low mass range). Because of its potentially large cross section on nuclei, it has been advocated as one of the possible explanations for the recent combined DAMA/NaI and DAMA/Libra results, ref. [16]. Such a candidate may be a source of gammas from the GC [16, 18] and neutrinos from the Sun [19, 20]. Here, we discuss the constraint posed on the IDM candidate by the limits from the Super-Kamiokande experiment.

However, the most natural dark matter candidate in the IDM has a mass $m_{DM} \sim 60$ GeV (middle mass range) [9, 11]. Furthermore, being a scalar, it has dominantly spin-independent interactions with nuclei. These features open the interesting possibility to enhance the capture of the IDM candidate by the Earth, through resonant scattering on heavy nuclei, in particular iron. This point has been already emphasized in [13], an article that appeared while our work was being completed. Our results on neutrinos and muons fluxes, obtained using different tools but making similar approximations regarding capture in the Earth, are in agreement. However, unlike in [13], we also take into account the constraints from direct detection experiments that lead to more pessimistic conclusions. In particular, we compare the flux of neutrinos with the expected sensitivity of IceCube, a km^3 neutrino telescope under construction at the South Pole, and show that this detector may at most give limits that are complementary, but not better than those given by existing and forthcoming dark matter direct detection experiments. In an attempt to improve this situation, we then consider a scenario based on a natural extension of the IDM with three generations of right-handed Majorana neutrinos. We show that, provided we somewhat depart from the scheme proposed in [8] for radiative SM neutrinos masses, some scalar candidates may have large annihilation rates into mono-energetic SM neutrinos, hence strongly boosting the possibility of observing indirect detection of dark matter captured by the Earth.

Finally, the IDM dark matter may be heavy, $m_{DM} \gtrsim 500$ GeV (high mass range) [11]. In this case, it has a very small cross section on nuclei and is therefore not likely to be captured by the Sun or by the Earth. On the other hand, it may accumulate at the centre of the Galaxy and its annihilation may produce high energy neutrinos that could be observed on Earth. However, we show that the flux is small for mundane astrophysical assumptions regarding the abundance of dark matter at the Galactic centre. Here, we set an upper bound on the neutrino flux that might be produced by assuming that the annihilation of the IDM candidate does not give gamma rays in excess of those observed by the EGRET satellite.

[1] This gives us a complete family of WIMPs. One should add the gravitino, a spin 3/2 state, and a spin 2 candidate might also exist in theories of modified gravity [7], or as a Kaluza-Klein partner of the graviton in theories with extra dimensions. These higher spin DM candidates have essentially gravitational interactions and are not WIMPs.

[2] This is a further step toward filling the gap in the table I given in ref. [17].

This paper is organized as follow. The Inert Doublet Model is introduced in section 2. In section 3, we fix our conventions on the dark matter abundance in the Galaxy, the Sun and the Earth. The section 4 is devoted to a review of capture and annihilation of WIMP dark matter in the Sun and in the Earth and their possible signatures in neutrino detectors or telescopes. In section 5, we envision the possibility of observing neutrinos produced at the Galactic centre. The predictions of the IDM are discussed in section 6, followed by our conclusions.

2 The Inert Doublet Model

The Inert Doublet Model is a two Higgs doublet model, H_1 and H_2, with an unbroken Z_2 symmetry under which

$$H_1 \to H_1 \ \text{ and } \ H_2 \to -H_2$$

and all the other Standard Model particles are even [8, 9]. The potential of the IDM can be written as

$$\begin{aligned} V &= \mu_1^2|H_1|^2 + \mu_2^2|H_2|^2 + \lambda_1|H_1|^4 + \lambda_2|H_2|^4 + \lambda_3|H_1|^2|H_2|^2 \\ &\quad +\lambda_4|H_1^\dagger H_2|^2 + \frac{\lambda_5}{2}\left[(H_1^\dagger H_2)^2 + h.c.\right]. \end{aligned} \tag{1}$$

In this model, H_1 contains the standard Brout-Englert-Higgs particle h (the Higgs for short) and the discrete symmetry, which prevents FCNC, gives a dark matter candidate in the form of one of the neutral components of the extra doublet $H_2 = (H^+, 1/\sqrt{2}(H_0 + iA_0))^T$. The couplings and masses of the scalar particles are related by

$$\begin{aligned} m_h^2 &= -2\mu_1^2 \equiv 2\lambda_1 v^2 \quad \text{with} \quad v = 246 \text{ GeV} \\ m_{H^+}^2 &= \mu_2^2 + \lambda_3 v^2/2 \\ m_{H_0}^2 &= \mu_2^2 + (\lambda_3 + \lambda_4 + \lambda_5)v^2/2 \\ m_{A_0}^2 &= \mu_2^2 + (\lambda_3 + \lambda_4 - \lambda_5)v^2/2\,. \end{aligned} \tag{2}$$

Depending on quartic couplings, either H_0 or A_0 can be the lightest Z_2-odd particle. We choose H_0 and, following [9], we define $\lambda_L = (\lambda_3 + \lambda_4 + \lambda_5)/2$, the coupling between h and a pair of H_0. In our investigation of the model we choose μ_2, λ_2 and the masses of scalar particles, including the Higgs, as input parameters.

Experimental constraints on the IDM model are discussed in [9] and further in [21] and [22]. The latter also discusses the prospect for discovery of the A_0 and H_0 at the LHC. In [21], the LEP I and II results on the neutralino are used to put constraints on the mass range of H_0 and A_0, see in particular their figure 8. In the present work, we consider that H_0 is the dark matter candidate. The A_0 masses (and that of $H^\pm$) we will use are always consistent with LEP data.

Assuming that H_0 were in thermal equilibrium in the early universe, there are essentially three distinct H_0 mass ranges that are consistent with the WMAP abundance for dark matter. In the sequel, we refer to them as the low mass (3 GeV $\lesssim m_{H_0} \lesssim$ 8 GeV), the middle mass (40 GeV $\lesssim m_{H_0} \lesssim$ 80 GeV), and the high mass (500 GeV $\lesssim m_{H_0} \lesssim$ 15 TeV) ranges.

Candidates in the low mass range annihilate only through the Higgs channel. These solutions may be compatible with the DAMA result [16], an hypothesis that may be tested in the future by other direct detection experiments (CDMS, XENON and CoGeNT). Candidates in the middle mass range annihilate in the Z (when coannihilation with A_0 is kinematically allowed) or the Higgs channel. Some solutions give a very significant gamma ray line from annihilation at the GC which might be observable with the GLAST/Fermi satellite [12]. Above 80 GeV, annihilation into $W^\pm$

pairs is allowed, the cross section is large and the abundance falls well below the WMAP abundance [11]. At higher masses, the annihilation cross section tends to decrease and the relic abundance increases. This regime is analogous to that of Minimal Dark Matter [23] but, in the IDM case, there are more parameters to play with and there is a whole mass range around 1 TeV of candidates with an abundance consistent with WMAP [11].

3 Dark matter distribution

The distribution of dark matter in the Galaxy is uncertain, in particular in the central region. Rotation curve observations suggest a rather cored profile [24, 25], with a flat behaviour at the centre, whereas numerical simulations predict more cuspy profiles in the innermost region of the Galactic centre (see Kravtov et al. [25], Navarro-Frenk-White (NFW) [26] and Moore et al. [27] as well as the recent Via Lactea and AQUARIUS simulations [28, 29]). Other studies even indicate the existence of a dark disk [30, 31]. In the present study, we will work with a fixed astrophysical framework and focus on the NFW profile which is parameterized as follows:

$$\rho(r) = \rho_0 \ \left(\frac{r}{r_0}\right)^{-\gamma} \left[\frac{1+(r_0/a_0)^\alpha}{1+(r/a_0)^\alpha}\right]^{\left(\frac{\beta-\gamma}{\alpha}\right)}, \tag{3}$$

where r_0 is the distance to the centre of the Galaxy, $\rho_0 = 0.3$ GeV/cm^3 is the dark matter density in the solar neighbourhood and (r_0 [kpc], a_0 [kpc], α, β, γ) = (8.5, 20, 1, 3, 1). In this framework, the dark matter halo is spherical and at rest in the Galactic coordinate system while the Sun moves on an orbit with mean velocity $v_\odot \approx 220$ km/s. The velocity of dark matter is supposed to have a Maxwell-Boltzmann distribution with mean velocity $\bar{v} = 270$ km/s.

4 Indirect detection from the Sun and the Earth

4.1 Capture rate

Dark matter of the Galactic halo might be captured in the Sun or the Earth due to the energy loss caused by elastic scattering of dark matter particles on nuclei. The size, density and composition of the Sun and the Earth are quite different and so is their ability to capture DM. WIMPs may generically couple with a nucleus through axial-vector (spin-dependent, SD) or scalar (spin-independent, SI) interactions [32]. In the latter case, elastic scattering with a nucleus is coherent and the cross section is proportional to the square of its atomic number A^2, while spin-dependent interactions depend only on the total spin of the nucleus $\sigma \propto J(J+1)$. The Sun is big and mainly composed of hydrogen atoms ($\sim 77\%$ of the mass of the Sun). Hydrogen is the lightest nucleus and therefore capture is likely to be more important for WIMPs with spin-dependent interactions. On the contrary, the Earth is comparatively small and mainly composed of heavy nuclei. Capture of dark matter particles may therefore be achieved by scalar spin-independent interactions.

Our treatment of capture in the Sun and the Earth will be elementary. Both for the sake of exploration and because, for the Earth, we will focus on a dark matter candidate in a mass range close to the iron mass, we follow the simple approximation of [33] and presented in the classical review [3]. This approach is expected to work for capture in the Sun. However, the situation for the Earth is more complex. The crux of the problem is that the Earth escape velocity is relatively small compared to the halo mean velocity, and in general capture in the Earth is sensitive to the (not well understood) low velocity part of the dark matter velocity distribution. The approximation of [33] and [3] consists in treating capture of dark matter from the halo as if the Earth was in free space.

However, the Earth is actually deep in the gravitational field of the Sun. Moreover, either through direct collisions or gravitational interactions, dark matter from the halo might be captured on solar bound orbits, possibly affecting the abundance and velocity distribution of dark matter particles near the Earth position. These and related issues have been investigated in details by Gould in [34] and further in [35], by Damour and Krauss [36], by Edsjö and Lundberg [37] and, more recently, by Peter [38, 39]. To make short a long, albeit fascinating story[3] – which implies taking into account the influence of planets – let us summarize here that these works show that the approximation we use for capture in the Earth works reasonably well if the dark matter candidate's mass is close to the iron resonance (see figure 16 of [37] and figure 10 of [39]), which is precisely the case we focus on in the present work. A more precise approach is clearly possible, for instance using the DarkSusy numerical package [40], but in the present work we have limited ourself to an analytical treatment both for capture in the Sun and in the Earth, an approach which, although not strictly speaking correct, is very simple to implement.

In the plain Inert Doublet Model, elastic scattering of H_0 with nuclei only takes place through Higgs exchange, which is a scalar, spin-independent interaction, figure 1.[4] The low energy cross section for spin-independent scattering of H_0 on a nucleus $\mathcal{N}_i$ of mass $m_{\mathcal{N}_i}$ is

$$\sigma^{SI}_{H_0\mathcal{N}_i\to H_0\mathcal{N}_i} \;=\; \frac{1}{\pi}\,\frac{\lambda_L^2}{m_h^4}\,\frac{m_{\mathcal{N}_i}^4}{(m_{H_0}+m_{\mathcal{N}_i})^2}\,f^2\,. \tag{4}$$

The factor f, that parametrizes the Higgs to nucleons coupling, is related to the trace anomaly, $f m_{\mathcal{N}} \equiv \langle\mathcal{N}|\sum_q m_q\bar{q}q|\mathcal{N}\rangle = g_{h\mathcal{N}\mathcal{N}}v$. This factor is not well known due to the uncertainty on the contribution of strange quarks to the nucleon's mass. From the results quoted in ref. [16], we take $f = 0.30$ as central value for a nucleon (we do not make a distinction between the coupling of the Higgs to a proton and a neutron) but it may be within a rather wide range $0.14 < f < 0.66$.

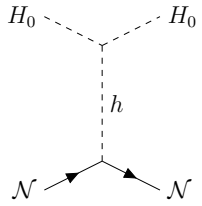

Figure 1: Scattering of H_0 on a nucleus $\mathcal{N}$ through exchange of a Higgs boson h.

The rate at which dark matter is captured by spin-independent scattering is given by,

$$C^{\odot/\oplus} \;=\; c_{\odot/\oplus}\,\frac{\rho_{local}}{0.3\ \mathrm{GeVcm^{-3}}}\,\frac{270\ \mathrm{km/s}}{\overline{v}_{local}}\,\sum_i F_i\,f_i\,\phi_i\,S_i\,\frac{\mathrm{GeV}^2}{m_{\mathcal{N}_i}\,m_{H_0}}\,\frac{\sigma_i}{10^{-40}\ \mathrm{cm}^2}, \tag{5}$$

where $c_\odot = 4.8 * 10^{24}\ \mathrm{s}^{-1}$ ($c_\oplus = 4.8 * 10^{15}\ \mathrm{s}^{-1}$) sets the scale for WIMP capture by the Sun (Earth), ref. [3].

The two astrophysical parameters, $\rho_{local} = 0.3$ GeV and $\overline{v}_{local} = 270$ km/s, refer to the local density and mean velocity of the dark matter halo. The sum runs over all elements present in the respective astrophysical object and encodes the information regarding their composition. The

[3] An historical summary, may be found in the article by Edsjö and Lundberg [37].

[4] For candidates in the middle and low mass ranges, inelastic scattering with Z boson exchange (*i.e.* $H_0 \to A_0$) is severely constrained by direct detection limits which impose $m_{A_0} - m_{H_0} \gtrsim 100$ keV [9].

parameters f_i and ϕ_i refer to the mass fraction and the distribution of element i. For those, we use the values given in [3].

The cross section for capture $\sigma_i = \sigma_i(m_{H_0}, m_{N_i})$ via spin-independent scattering on nuclei at low momentum transfer is given by eq. (4). The $F_i = F_i(m_{H_0})$ are nuclear form factors and the suppression factor $S_i = S_i\big(\frac{m_{H_0}}{m_{N_i}}\big)$ encodes the kinematics of DM-nuclei elastic collisions. Capture in the Earth is greatly enhanced by the appearance of resonances between the masses of the nuclei and of the WIMP. For the discussion, it is useful to introduce the dimensionless parameter $x = m_{H_0}/m_{\mathcal{N}_i}$. The effect of resonances can be understood from an interplay of two factors: the kinematic suppression S_i and the form-factor suppression F_i. The kinematic suppression factor S is defined as:

$$S(x) \;=\; \Big[\,\frac{A^{3/2}}{1\,+\,A^{3/2}}\Big]^{2/3}, \qquad \text{with} \qquad A(x) \;=\; \frac{3}{2}\,\frac{x}{(\,x\,-\,1)^2}\,\Big(\,\frac{\langle\, v_{esc}^2\,\rangle}{\bar{v}_{local}^2}\,\Big), \tag{6}$$

where $\langle\, v_{esc}^{\odot}\rangle = 1156$ km/s ($\langle\, v_{esc}^{\oplus}\rangle = 13.2$ km/s) is the Sun (Earth) escape velocity.

The behaviour of S depends on the escape velocity and therefore differs for Sun and Earth. S asymptotically scales like A when $A \to 0$ while $S \to 1$ for $A \to \infty$. A is strongly peaked when the WIMP's mass matches a nucleus' mass ($x \to 1$). For the Sun, the higher escape velocity brings A above 1 in all but a few extreme points (small m_{H_0}) for all elements except hydrogen. Because of this behaviour, $S \simeq 1$ in the biggest part of the mass range. However, in the case of the Earth, $A \ll 1$ almost everywhere except at the resonances. Therefore, $S \simeq 1$ only in a small region around the resonance while elsewhere $S \sim A \ll 1$.

The nuclear suppression form factor takes into account the fact that nuclei are made of nucleons. If both the WIMP's kinetic energy in the halo and its maximum energy transfer to the nucleus are comparable to the characteristic coherence energy, the WIMP sees the substructure of the nucleus and the cross section is reduced. For the Earth, it can be derived [41] that this effect is only relevant at the resonances and that the suppression is negligible (5% effect) for all elements except iron. Therefore, following [3], we assume that the form factor suppression is 1 for all elements but iron for which it is parameterized as

$$F_{\mathrm{Fe}} \;=\; 1 \,-\, 0.26\frac{A}{1+A}\,. \tag{7}$$

In the case of capture by the Sun, one has to take into account that the kinetic energy of the WIMP when scattering on a nucleus is not anymore the kinetic energy at infinity (connected with the local velocity in the halo) but receives a contribution from the Sun's gravitational potential. It can then be shown that the form-factor suppression is no longer confined to the resonances and additionally that it applies to all elements [3]:

$$F_i \;=\; F_i^{inf} \,+\, (1 - F_i^{inf})\,\exp\Big[\,-\,\Big(\frac{\log m_{H_0}}{\log m_c^i}\Big)^{\alpha_i}\Big] \tag{8}$$

except for hydrogen, where $F = 1$. Therein F_i^{inf}, m_c^i and α_i are fit parameters tabulated in [3]. The form-factor in the Sun has basically no effect on the lightest elements (hydrogen and helium) while for heavier nuclei it leads to a suppression which is increasing with the mass of the element. Capture on iron experiences the strongest suppression, $\mathcal{O}(10^{-1} - 10^{-2})$ for the heaviest dark matter candidates in the middle range under consideration.

To summarize the dependence on the WIMP's mass and the different nuclei, we define for the IDM candidate a function $\mathcal{F}_{\odot/\oplus}$

$$\mathcal{F}_{\odot/\oplus} = \sum_i f_i^{\odot/\oplus}\phi_i^{\odot/\oplus} S\big(\frac{m_{H_0}}{m_{\mathcal{N}_i}}, v_{esc}^{\odot/\oplus}\big)\, F_i^{\odot/\oplus}(m_{H_0}, \mathcal{N}_i)\,\frac{m_{\mathcal{N}_i}^3}{(m_{H_0}+m_{\mathcal{N}_i})^2}\,\frac{\lambda_L^2}{m_{H_0} m_h^4}\,f^2\,\frac{\mathrm{GeV}^2}{10^{-40}\ \mathrm{cm}^2}. \tag{9}$$

The behaviour of $\mathcal{F}_{\odot/\oplus}$ as a function of m_{H_0} is displayed in figure 2 both for the Earth and the Sun. It shows in particular the great importance of the iron resonance in the case of the Earth. With the definition of $\mathcal{F}_{\odot/\oplus}$, the capture rate can be written:

$$C^{\odot/\oplus} \;=\; \frac{c_{\odot/\oplus}}{\pi}\;\frac{\rho_{local}}{0.3\ \mathrm{GeV\ cm^{-3}}}\;\frac{270\ \mathrm{km/s}}{\overline{v}_{local}}\;\mathcal{F}_{\odot/\oplus}. \tag{10}$$

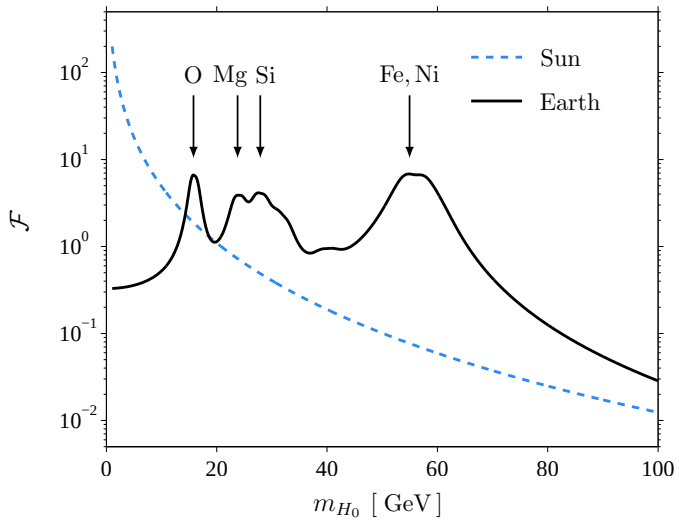

Figure 2: Typical behaviour of $\mathcal{F}_{\odot/\oplus}$ in function of m_{H_0} for Sun (dashed blue line) and Earth (solid black line). The resonance phenomenon, which is present for elements in the Earth, is absent for the Sun (here for $m_h = 120$ GeV, $f = 0.3$ and $\lambda_L = 0.2$).

4.2 Annihilation rate

The number N of WIMP dark matter in the Sun or Earth is controlled by the capture and annihilation rates

$$\frac{dN}{dt} \;=\; C \;-\; 2\,\Gamma, \tag{11}$$

where C is the capture rate defined in eq. (5) and Γ is the annihilation rate. For a self conjugate particle, like H_0, the total annihilation rate from a (effective) volume V_{eff} is given by

$$\Gamma \;=\; \frac{N^2}{2V_{\mathrm{eff}}}\,\sigma v. \tag{12}$$

The cross section for annihilation of H_0 is through the Higgs channel only, figure 3, and is given by

$$\sigma|\vec{v}|_{H_0H_0\to f\bar{f}} \;=\; \frac{n_c}{\pi}\;\frac{\lambda_L^2}{(\,4\,m_{H_0}^2 \,-\, m_h^2\,)^2}\;\frac{m_f^2\,(\,m_{H_0}^2 \,-\, m_f^2\,)^{3/2}}{m_{H_0}^3}\,. \tag{13}$$

With eq. (12) the solution of (11) is

$$\Gamma \;=\; \frac{C}{2}\,\tanh^2\Big(\sqrt{\frac{\sigma v}{V_{\mathrm{eff}}}\,C}\;t_\odot\Big) \;=\; \frac{C}{2}\,\tanh^2\left(t_\odot\,/\,\tau\right) \;=\; \frac{C}{2}\,F_{\mathrm{EQ}}, \tag{14}$$

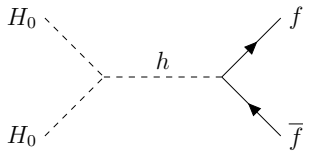

Figure 3: The only tree level annihilation channel of light H_0 ($m_{H_0} \lesssim m_W$) into fermions pairs is through the Higgs boson.

where

$$F_{\rm EQ} \;=\; \tanh^2\left(\, t_\odot \,/\, \tau \,\right) \qquad \text{and} \qquad \tau \;=\; \sqrt{\frac{V_{\rm eff}}{\sigma v\, C}}, \tag{15}$$

and $t_\odot = 4.5$ Gyr is the age of the solar system. The effective volume of the Sun or of the Earth is determined by roughly matching the core temperature with the gravitational potential energy of the WIMP at the core radius. Following [3, 41, 42] we adopt

$$V_{\rm eff}^{\odot} \;=\; 5.8 * 10^{30}\ {\rm cm}^3 \left(\frac{\rm GeV}{m_{H_0}}\right)^{3/2}, \tag{16}$$

$$V_{\rm eff}^{\oplus} \;=\; 1.8 * 10^{27}\ {\rm cm}^3 \left(\frac{\rm GeV}{m_{H_0}}\right)^{3/2}. \tag{17}$$

If the time scale τ for capture and annihilation to equilibrate is small compared to the age of the solar system, the equilibrium factor and annihilation rate reach a maximum, $t_\odot \gg \tau \;\Rightarrow\; F_{\rm EQ} = 1 \;\Rightarrow\; \Gamma = C/2$.

Given Γ, the differential flux of annihilation products i in the Sun or Earth is given by

$$\left(\frac{d\phi}{dE}\right)_i \;=\; \frac{\Gamma}{4\pi R^2} \sum_F BR_F \left(\frac{dN}{dE}\right)_{F,i} \tag{18}$$

$$\;=\; \frac{1}{2}\,\frac{C\,F_{\rm EQ}}{4\pi R^2} \sum_F BR_F \left(\frac{dN}{dE}\right)_{F,i}, \tag{19}$$

where R is either the distance from the Sun to the Earth ($R = d_{\odot-\oplus} = 1.5 * 10^8$ km) or the radius of the Earth ($R = r_\oplus = 6300$ km). BR_F is the branching ratio for annihilation into final state F and $(dN/dE)_{F,i}$ is the differential spectrum of the annihilation products i through the decay channel F. The sum on F runs over all the kinematically allowed final states.

4.3 Muon flux

In the following, only the resulting flux of muonic neutrinos will be taken into account, since they provide the best directional information. Electron- or tau-neutrinos produce a particle shower close or within the detector volume hence blurring the directional information.

For neutrinos from dark matter annihilation, one may distinguish two extreme cases referred to as soft and hard spectra. The soft spectrum is falling rapidly with the neutrino energy. The hard spectrum on contrary is flatter with significant contributions at high energies. Specifically, annihilations of H_0 into $b\overline{b}$ quarks give a soft spectrum of neutrinos, while a hard spectrum originates either from pairs of W or Z bosons (if $m_{H_0} \gtrsim m_W$) or from $\tau^+\tau^-$ (if $m_{H_0} < m_W$) channels.

The detection rate per unit detector area of neutrino-induced, through-going muon events from the Sun or the Earth is computed using the charged-current cross sections and the muon range. Ignoring detector thresholds, as in reference [3], the muon flux in the detector is found to be:

$$\phi_\mu^{\odot/\oplus} \;=\; \varphi_{\odot/\oplus} \;\; \frac{C^{\odot/\oplus}\, F_{\rm EQ}}{2\ {\rm s}^{-1}} \left(\frac{m_{H_0}}{\rm GeV}\right)^2 \sum_i a_i\, b_i \sum_F BR_F \,\langle\, N z^2 \rangle_{F,i}\,(m_{H_0}), \tag{20}$$

where $\varphi_\odot = 2.54 * 10^{-23}\ {\rm km}^{-2}\ {\rm yr}^{-1}$ ($\varphi_\oplus = \varphi_\odot\ (d_{\odot-\oplus}/r_\oplus)^2 = \varphi_\odot * 5.6 * 10^6$) for the Sun (Earth), $C^{\odot/\oplus}$ is the capture rate defined in eq. (5, 10) and $F_{\rm EQ}$ is the equilibrium factor defined in eq. (15). The neutrino-scattering coefficients a_i and muon-range coefficients b_i are given in [3] as $a_\nu = 6.8$, $a_{\overline{\nu}} = 3.1$, $b_\nu = 0.51$ and $b_{\overline{\nu}} = 0.67$. BR_F is the branching ratio for annihilation into final state F and $\langle\, N z^2 \rangle_{F,i}(m_{H_0})$ is the second moment of the spectrum $(dN/dE)_{F,i}$ of neutrinos of type i from final state F scaled by the square of the injection energy E_{in}

$$\langle\, N\, z^2 \,\rangle_{F,i}\,(E_{in}) \;=\; \frac{1}{E_{in}^2} \int \left(\frac{dN}{dE}\right)_{F,i} (E_\nu, E_{in})\, E_\nu^2\, dE_\nu. \tag{21}$$

As neutrino detectors have certain thresholds on the minimum neutrino energy detectable, a lower, detector dependent, energy bound is implicit in the integration range.

5 Indirect detection from the Galactic centre

Simulations indicate that there is a higher dark matter density at the centre of the Milky Way. As for the Sun and the Earth, this opens the possibility of indirect detection of dark matter through its annihilation products. The expected flux from the Galactic centre depends on the assumed dark matter density profile ρ.

For a self conjugate dark matter candidate, like the H_0, the flux of annihilation products i at the Earth is

$$\frac{d\phi_i}{dE} \;=\; \frac{1}{2}\, r_0\, \rho_{local}^2\, \frac{dN_i}{dE}\ \ \frac{\sigma v}{4\pi m_{H_0}^2}\ \ \overline{J}(\Delta\Omega)\ \Delta\Omega, \tag{22}$$

$$\text{with} \quad \overline{J}(\Delta\Omega) \;=\; \frac{1}{\Delta\Omega}\, \frac{1}{r_0\, \rho_{local}^2} \int_{\Delta\Omega} d\Omega \int_{\text{line of sight}} ds\ \ \rho^2(r(s,\theta)), \tag{23}$$

where $r_0 = 8.5$ kpc is the distance to the Galactic centre, dN/dE is the energy spectrum of annihilation products and σv is the total annihilation cross section times velocity. The factor $1/2$ results from the number of ways to have a pair out of n particles $\sim n^2/2$.[5] The quantity $\overline{J}$ encompasses all the astrophysics and is defined as the integral of $\rho^2(r)$ along the line of sight averaged over a solid angle $\Delta\Omega$. With a NFW profile, the integration gives for instance $\overline{J} = 1382$ for $\Delta\Omega = 10^{-3}$, corresponding to the resolution of EGRET, or $\overline{J} = 536$ for $\theta = 2.5°$, which is the resolution of ANTARES, a neutrino telescope which is able to look in the direction of the Galactic centre.

6 IDM results

Our discussion is divided into the three mass ranges for the H_0 candidate. In each case, the relevant astrophysical context is distinct.

[5] This factor of 1/2 is in agreement with the expression given by [17], [43] and [44].

6.1 Low mass candidate: indirect detection from the Sun

The light dark matter candidate $m_{H_0} < 10$ GeV of the IDM has been studied in [16] in view of explaining the DAMA annual modulation signal. Such a candidate has a larger number density than heavier candidates. It is however too light to give a large signal from the core of the Earth (see figure 2). Because of its large number density and quite large cross section, annihilations at the Galactic centre might be important and, indeed, a large flux of photons is to be expected which might be studied by the GLAST/Fermi satellite [16, 18]. At these energies, however, the flux of neutrinos is well below the background of atmospheric neutrinos. The only possible relevant source of neutrinos might thus be the Sun.

The result of our analysis, for $m_h = 120$ GeV, is given in figure 4 where we show both the expected flux of muonic neutrinos according to eq. (19) and that of muons from eq. (20) as a function of the mass of the dark matter candidate, m_{H_0}, and the bare mass scale, μ_2. The neutrino spectra have been computed using WimpSim [45, 46][6] and are cut at a threshold energy $E_\nu = 2$ GeV. The fluxes are shown together with the WMAP allowed region in black (which we have computed using micrOMEGAs [47]) for $0.094 < \Omega_{DM} h^2 < 0.129$, the current limits set by direct detection experiments (in white, from left to right, XENON and CDMS respectively) and the DAMA allowed region (in light blue) for $f = 0.3$ (cf. ref. [16], the allowed region remaining after exclusions of all other direct searches).

As emphasized in [20] and [48], the flux of neutrinos produced in the Sun by such a light DM candidate might be constrained by the Super-Kamiokande experiment. Its sensitivity is currently only set down to $m_{DM} = 18$ GeV from studies of through-going muons [49]. It could however be extended down to 2 GeV including stopping, partially contained or fully contained muons [20]. In the present work, the estimation of the Super-Kamiokande sensitivity (drawn in blue) has been obtained horizontally extrapolating the one given in [49] to lower DM masses. This limit has been rescaled to a muon threshold of 1 GeV (cf. [50]) which corresponds to the neutrino threshold $E_\nu = 2$ GeV assuming an energy loss of $\simeq 50$ % in the neutrino to muon conversion. Compared to the projected Super-Kamiokande sensitivity presented in [20], our extrapolation is more conservative.

Since $m_{H0}^2 = \mu_2^2 + \lambda_L v^2$, a light H_0 and μ_2 in the range of both DAMA and WMAP require a large, negative coupling λ_L within $\sim [-0.6, -0.1]$. This in turn requires a rather large λ_2 to insure the stability of the potential. Concretely one needs [9]

$$\lambda_2 \; > \; \lambda_L^2 \; / \; \lambda_1 \; \equiv \; \frac{2(m_{H_0}^2 - \mu_2^2)^2}{v^2 m_h^2}. \tag{24}$$

for $\lambda_{1,2} > 0$ and $\lambda_L < 0$. In figure 4, the shaded regions correspond to a coupling $\lambda_2 > 1$, for $m_h = 120$ GeV. In the low mass range, both the annihilation and the capture cross section are proportional to $\lambda_L^2/m_h^4 \propto \mu_2^4/m_h^4$ ($\lambda_L \propto \mu_2^2$), cf. equations (4) and (13). When increasing the Higgs mass, this ratio must be kept constant not to reduce the neutrino/muon flux. The Super-Kamiokande sensitivity is therefore shifted to higher values of μ_2 that are increased $\propto m_h$. On the other hand, the displacement of the exclusion limit $\lambda_2 > 1$ is only $\propto \sqrt{m_h}$. The sensitivity lying for $m_h = 120$ GeV in the $\lambda_2 > 1$ region will require even larger values of λ_2 for higher Higgs masses.

Figure 4 shows that Super-Kamiokande is potentially able to test the light IDM candidate and a part of the DAMA allowed region (from about 3 GeV to 4.8 GeV). However, the required couplings tend to be rather large.

A similar conclusion is found adapting the analysis of ref. [48] which gives the limit set by Super-Kamiokande assuming a DM candidate that annihilates with branching ratio = 1 either into $\tau - \overline{\tau}$,

[6] To take into account the effect of neutrino oscillations, we take the flux of muon neutrinos at the Earth to be equal to one third of the total flux of neutrinos produced at the core of the Sun.

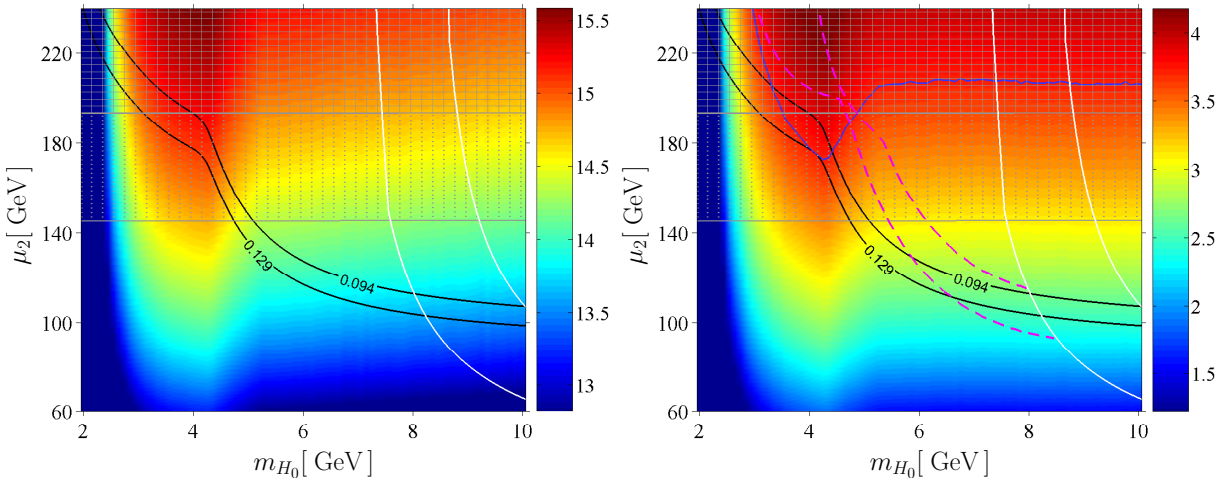

Figure 4: Expected neutrino (*left*) and muon (*right*) fluxes from the Sun, for a neutrino energy threshold of 2 GeV. Dark blue line in the muon flux plot: estimate of Super-Kamiokande sensitivity, conservatively extrapolated to light WIMPs (see text).
Colour gradient - $\log_{10}\phi_\nu$ $[km^{-2}\,yr^{-1}]$ *(left) and* $\log_{10}\phi_\mu$ $[km^{-2}\,yr^{-1}]$ *(right); WMAP area (black lines); DAMA allowed region (dashed magenta lines); XENON, CDMS exclusion limits (white lines, from left to right); The shaded regions correspond to* $\lambda_2 > 1$.
(Parameters: $m_h = 120\,GeV$, $\lambda_2 = 1$ *(dotted) and* $\lambda_2 = \pi$ *(shaded),* $f = 0.3$*).*

$c - \bar{c}$ or $b - \bar{b}$ pairs, the strongest constraint being for annihilations into τ leptons. This limit for $\tau^+\tau^-$ rescaled by the actual branching ratio in the frame of the IDM is shown in figure 5 (in blue) together with the DAMA allowed region (in light blue) and other direct detection experiments (in green).

For the H_0 candidate, the limit from the tau channel indicates (in agreement with the result of figure 4) that the limit set by Super-Kamiokande is competitive with limits set by direct detection experiments (modulo the uncertainties regarding the abundance of dark matter in the Sun versus that at the Earth, as usual).

6.2 Middle mass candidate: indirect detection from the Earth

This refers to a H_0 with a mass typically between 40 and 80 GeV [11]. Since the H_0 has essentially spin-independent interactions, the best place to look for neutrinos produced in annihilations is toward the centre of the Earth. However, direct detection experiments put very stringent limits on the SI cross section of WIMPs and so on the potential signatures in neutrino telescopes.

In this section, we discuss the muon flux resulting from H_0 annihilations in the Earth. First we consider the Inert Doublet Model in its most minimalistic version and show that some of the candidates that have an abundance in agreement with WMAP give a muon flux that almost reaches the sensitivity of a km size detector like IceCube. We then consider two extensions. First we discuss the possible effect of one-loop corrections, in the spirit of [12] but conclude that they may not significantly improve the signatures of the IDM into neutrinos. Finally, we consider the extension of the IDM with three heavy Majorana neutrinos introduced in [8]. This extension opens the possibility of annihilations of H_0 into two SM ν or two $\bar{\nu}$ with energy $m_{\nu,\bar{\nu}} = m_{H_0}$, thus strongly (albeit to the price of some fine tuning) increasing the potential signature in neutrino telescopes.

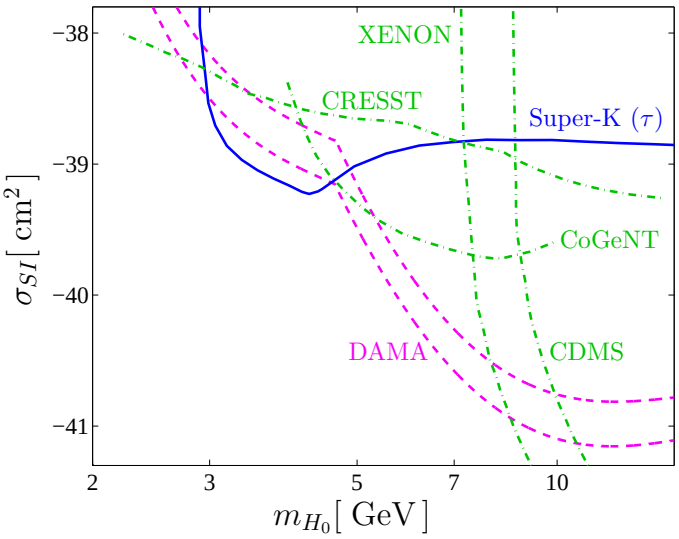

Figure 5: The region allowed by DAMA (dashed magenta lines) together with limits on the spin-independent elastic scattering cross section of H_0 on a nucleus from direct detection experiments (dash-dotted green lines), cf. [51]. Super-Kamiokande (solid blue line) sets another limit from the $\tau^+\tau^-$ annihilation channel of H_0. This limit results from the one presented in [48] rescaled by the IDM branching ratio.

6.2.1 The minimal scenario

Applying the results of section 4.3, the muon flux is given by (14). For SI scattering, the Earth is expected to have a higher capture rate for dark matter masses near the main resonances. In the range of H_0 masses under consideration, the dominant resonance is that of iron. The expected muon flux is presented in figure 6 for four different Higgs masses. In this figure, we neglect the effect of detector thresholds and give the total flux of muons. Hence, this is the maximal signal that one may get, of course assuming standard hypotheses regarding the abundance of dark matter at the centre of the Earth. The mass splittings for A_0 and $H^\pm$ (8 and 50 GeV respectively) are consistent with LEP data [21].

The figures show the muon flux (colour gradient) together with the 2σ WMAP abundance region. The shaded regions are excluded by stability considerations and the LEP I limit on the Z width. We give the limit (in white) imposed by direct detection experiments (*i.e.* CDMS and XENON [52]). Finally, the sensitivity of the IceCube detector is shown in blue. It depends on the neutrino spectrum, for which a distinction between so-called 'hard' and 'soft' spectra is made. The former results from annihilation channels like $\tau^+\tau^-$, the latter from $b\bar{b}$ pairs. For the Earth, the IceCube best case sensitivity for $m_{DM} = 50$ GeV is ~ 15 muons per km^2 yr for a hard spectrum and ~ 40 muons per km^2 yr for a soft spectrum. Here we adopt the best case sensitivity presented for example in [50] as a function of m_{DM} for 50 GeV $< m_{H_0} <$ 100 GeV and its extrapolation down to candidates with a mass of 30 GeV. Since the dominant annihilation channel is into $b\bar{b}$, we use the sensitivity for a soft spectrum.

Annihilation rates and thus muon fluxes are higher for candidates with a mass close to $m_h/2$. This however gives a cosmic abundance too low compared to WMAP. This tension resolves as the mass of the Higgs is increased. Our results are in agreement with those of [13]. However, we find that the candidates with a potential signature in IceCube correspond to regions of parameters that are not favoured since they either give a too small abundance ($m_h = 120$ GeV and 140 GeV), or

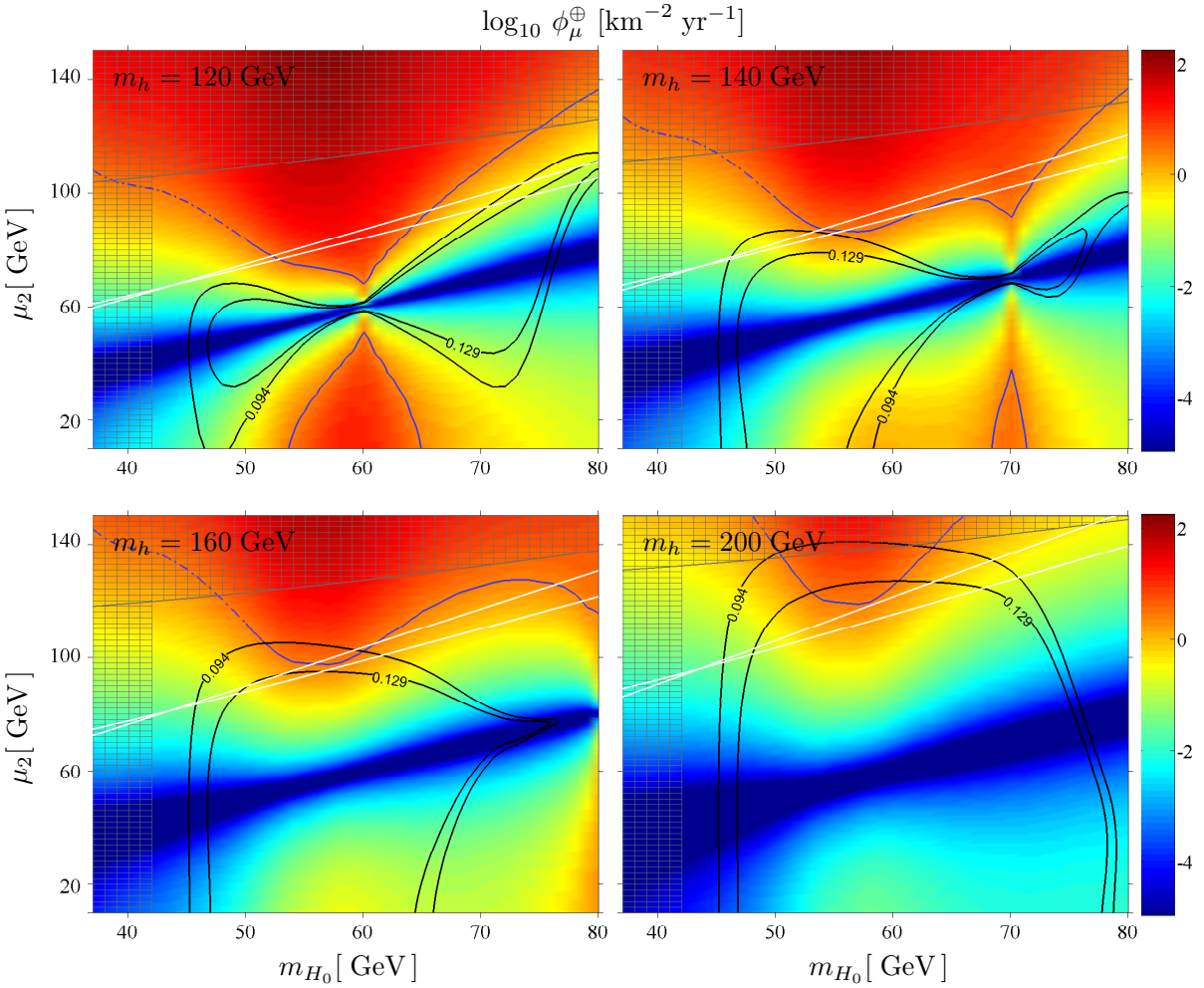

Figure 6: Muon flux from the Earth for the minimal scenario (see text). No detector threshold is applied.
Colour gradient - $\log_{10}\phi_\mu$ $[\mathrm{km}^{-2}\,\mathrm{yr}^{-1}]$*; WMAP area (black lines); XENON, CDMS exclusion limits (white lines); IceCube sensitivity soft (blue lines); excluded regions (shaded).*
(Parameters: $\lambda_2 = 0.2$, $\Delta m_{A_0 H_0} = 8\,GeV$, $\Delta m_{H^+ H_0} = 50\,GeV$, $f = 0.3$*).*

are within the exclusions limits set by current direct detection experiments ($m_h = 160$ GeV and 200 GeV). For the sake of completeness, we illustrate the variation of the muon flux obtained by varying the Higgs-nucleon coupling form factor f in figure 7.

For small values of f, a part of the parameter space with muon flux above the sensitivity is in agreement with direct detection. This region is however outside the 2σ WMAP area. Relaxing the WMAP limit on the abundance (acceptance obtained with the 3σ WMAP area) could give a muon flux above the IceCube sensitivity for some candidates that are not yet excluded by direct detection experiments.

6.2.2 A non-minimal scenario: effect of loop corrections

To increase the flux of muons one possible strategy is to envision candidates with a hard(er) neutrino spectrum, thus exploiting the fact that the muon flux is $\propto E_\nu^2$, eq. (20). The best case is to have

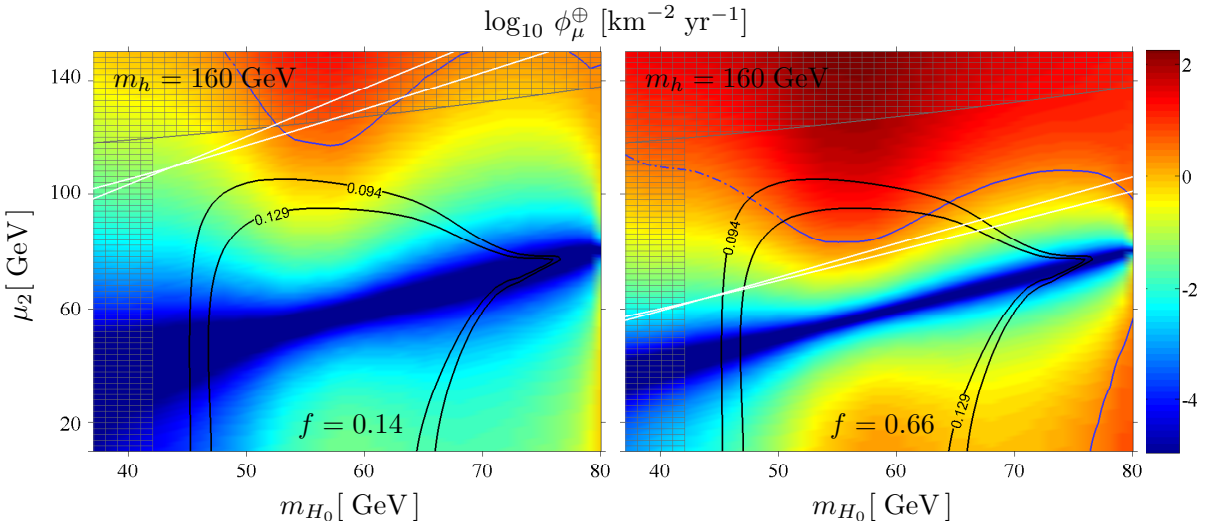

Figure 7: Muon flux from the Earth for the minimal scenario for different values of the factor f. The figure comes from the down-left plot in figure 6, when varying f. No detector threshold is applied.
Colour gradient - $\log_{10}\phi_\mu$ [km^{-2} yr^{-1}]; *WMAP area (black lines); XENON, CDMS exclusion limits (white lines); IceCube sensitivity soft (blue lines); excluded regions (shaded).*
(Parameters: $\lambda_2 = 0.2$, $\Delta m_{A_0 H_0} = 8\,GeV$, $\Delta m_{H^+ H_0} = 50\,GeV$, $f = 0.14$ *(left) and* $f = 0.66$ *(right)).*

annihilations into mono-energetic neutrinos, a solution that we will consider in section 6.2.3. First we consider the possibility that H_0 may annihilate into $\gamma - \bar{\nu}\nu$ at one-loop.

At one loop the H_0 may annihilate into a pair of photons ($\gamma\gamma$) or into a photon and a Z boson (γZ). The relevance of these contributions in the IDM model has been emphasized in [12]. In turn, the Z may decay into $\nu\bar{\nu}$. There is another contribution, through a loop with W-bosons, for annihilation into $\nu\bar{\nu}\gamma$. This contribution has not yet been computed in the literature. Here, to explore whether it would be worth being computed, we make the reasonable assumption that this contribution does not overwhelm that from Z decay. The energy at which the Z boson is produced is $E_Z = m_{H_0} + m_Z^2/4m_{H_0}$ if $m_{H_0} > m_Z/2$ and the spectrum of neutrinos is peaked around $E_Z/2$.

In [12], the possibility of direct annihilation into photons and Z bosons has been investigated in view of observing gamma rays from the Galactic centre and four benchmark models (BM), shown here in table 1, are proposed.

To compute the expected muon flux for those BMs, all we need is the decay spectrum of a Z boson in addition to the information given in table 1. For a Z with an energy E_Z, the neutrino spectrum is obtained using WimpSim. The muon flux for each benchmark model is then calculated with eq. (20) using the branching ratios of table 1.

The BMs have specific parameters combinations which are optimized to give the right WMAP abundance, not specially a large flux of Z and by consequence not a large muon flux from the Earth (BM I has a large branching ratio into a Z, but a relatively small annihilation cross section). For this, we need, ideally, a large branching ratio into γZ (like BM I and III) and a large annihilation cross section (BM IV and, to lesser extent, BM III). Additionally, a large cross-section via the Higgs is required (BM IV and III again) so that capture in the Earth through SI interaction is efficient, cf. eq. (4) and figure 1. Finally, we want a dark matter mass close to the iron resonance. BM III realizes the best compromise, but even in this case the flux is below the sensitivity of IceCube. The

signature in gamma rays from the GC, as envisioned in [12], may benefit from the possibility of introducing a boost factor (BF), taking into account the uncertainty regarding the abundance of dark matter at the GC. Although, with a bit of luck, a signal in gamma rays could be seen even without a BF, with BF$= 10^2 - 10^4$, the signature would be spectacular. Such a BF may be possible at the GC but is unlikely in the Solar system vicinity, and *a fortiori* in the Earth.

	Benchmark Model	**I**	**II**	**III**	**IV**
Parameters [GeV]	m_h	500	500	200	120
	m_{H_0}	70	50	70	70
	m_{A_0}	76	58.5	80	80
	m_{H^+}	190	170	120	120
	μ_2	120	120	125	95
	$\lambda_2 * 1$ GeV	0.1	0.1	0.1	0.1
	Ωh^2	0.1	0.1	0.12	0.11
	σv_{tot} [cm^{-3} s^{-1}]	1.6e-28	8.2e-29	8.7e-27	1.9e-26
Branching Ratio [%]	γ Z	33	0.6	2	0.1
	$\gamma\gamma$	36	29	2	0.04
	$b\bar{b}$	26	60	81	85
	$c\bar{c}$	2	4	5	5
	$\tau^+\tau^-$	3	7	9	10
Muon rate [km^{-2} yr^{-1}]	$\gamma - Z$ only	4.12e-06	1.82e-06	3.36e-02	4.75e-03
	$\gamma - Z$ + tree level	4.81e-06	2.63e-05	3.16e-01	8.58e-01

Table 1: Parameters and branching ratios for the four IDM benchmark models presented in [12]. The maximum muon fluxes assuming no detector thresholds are far below the sensitivity of IceCube.

6.2.3 Another non-minimal scenario: introducing Majorana neutrinos

A natural extension of the IDM model consists in the addition of right-handed Majorana neutrinos, odd under Z_2 [8]. This introduces the possibility to give a mass to the SM neutrinos through radiative corrections. The IDM Lagrangian then contains additional terms,

$$\mathcal{L} \supset h_{ij}\,(\nu_i\,H_0 - l_i\,H^+)N_j + \frac{1}{2}M_j N_j N_j + h.c. \tag{25}$$

where the index i stands for the SM neutrino generation ($i = e, \mu, \tau$) and j for the three extra Majorana neutrinos ($j = 1, 2, 3$). Further discussion about the generation of neutrino masses can be found in [8]. In this extension of the IDM, the dark matter candidate may be either a boson, the lighter of the two neutral components of the H_2 doublet (H_0 or A_0), or a fermion, if one of the Majorana neutrinos is the lightest odd particle. As in the previous sections, we take the H_0 as dark matter candidate and focus on the fact that the direct coupling between H_0 and SM neutrinos allows annihilations of H_0 into pairs of SM neutrinos or antineutrinos, with $E_{\nu,\bar{\nu}} = m_{H_0}$, see figure 8. In principle, annihilation into $\nu\bar{\nu}$ is also possible. However, this process is either p-wave suppressed, $\propto v_{\rm rel}^2$, or helicity suppressed, $\propto m_{\nu_i}^2$. The cross section for annihilation into $\nu\nu$ or the conjugate channel, $\bar{\nu}\bar{\nu}$, is of the form

$$\sigma|\vec{v}| \;=\; \frac{h^4}{4\pi}\;\frac{m_N^2}{(m_{H_0}^2 + m_N^2)^2}\,. \tag{26}$$

To simplify our, exploratory level, discussion we focus on muonic neutrinos and suppose that only one Majorana neutrino, with mass m_N, enters the cross section. We do not consider the possibility of oscillations, which is a good approximation for the Earth. For reference, from here on we take $m_N = 100$ GeV and set the Yukawa coupling to $h = 0.1$. These values are chosen so as to boost the signal into mono-energetic neutrinos, which requires a rather light Majorana neutrino. At the same time the SI cross section has to be large enough to ensure efficient capture in the Earth. Meeting all these constraints requires some fine tuning, but is possible for a broad range of parameters.

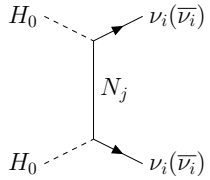

Figure 8: Direct annihilation of H_0 into neutrinos ν_i (or antineutrinos $\overline{\nu}_i$) through exchange of a Majorana neutrino N_j leading to a mono-energetic neutrino flux.

The total muon flux coming only from annihilations into mono-energetic neutrinos is shown in figure 9, for different Higgs masses. The plotted IceCube sensitivity curves (blue lines) are the ones for a hard neutrino spectrum. The abundance used for the WMAP limit (black lines) has been computed with micrOMEGAs. Note that the shape of the WMAP regions differs from the ones of figure 6 as annihilations into neutrinos or antineutrinos are also relevant at freeze-out.

For all Higgs masses but $m_h = 120$ GeV, there is a region of the parameter space that is in agreement with WMAP and for which the muon flux is above the IceCube sensitivity. As in the previous sections, uncertainties in f affect the muon flux. We have set $f = 0.3$ but spanning over the range of f preserves the overlap observed, for example, for $m_h = 200$ GeV while an increase of f for $m_h = 120$ GeV brings the WMAP region within the IceCube sensitivity curve.

Figure 10, which is a scattered plot over parameters of the model, gives the total muon flux from the Earth in function of the DM mass. The left panel shows that for the IDM several points above the IceCube sensitivity are in agreement with both WMAP and direct detection. Additionally, for the sake of comparison, the muon fluxes for the MSSM are shown in the right panel. The interesting IDM candidates are peaked around the iron resonance (50 GeV $< m_{H_0} <$ 60 GeV). For parameters in agreement with WMAP (dark blue points for the IDM, yellow ones for the MSSM), the IDM fluxes are typically about 2 orders of magnitude larger than the MSSM ones and well above the IceCube sensitivity. Actually, there are even a few points that are within the sensitivity of Super-Kamiokande.

On the negative side, we have to face the fact that a boost of the signal into mono-energetic neutrinos requires a rather light Majorana particle ($m_N \sim 100$ GeV) and a coupling to SM neutrinos of the order $h \sim 0.1$. For those values of the parameters, similar to those used in [53], the one-loop contribution to the masses of the SM neutrinos is quite large, $m_\nu \sim$ keV range, which clearly contradicts the current limits on neutrino masses [54]. One way around is to make use of the fact that the absolute sign of fermions is non-observable and to assume that there is another contribution to the SM neutrino masses, beyond the IDM (say through non-renormalisable operators) that compensates the contribution from the light Majorana neutrino. Albeit this is contrived in our case, as it would require a fine tuning of parameters at least at level 10^{-3}, a similar mechanism is sometimes invoked, for instance in supersymmetric models with a sneutrino as the dark matter candidate [55]. Presumably, we should also make sure that no other dangerous radiative processes are important, like $\mu \to e + \gamma$ [53]. This is, however, beyond the scope of the present work.

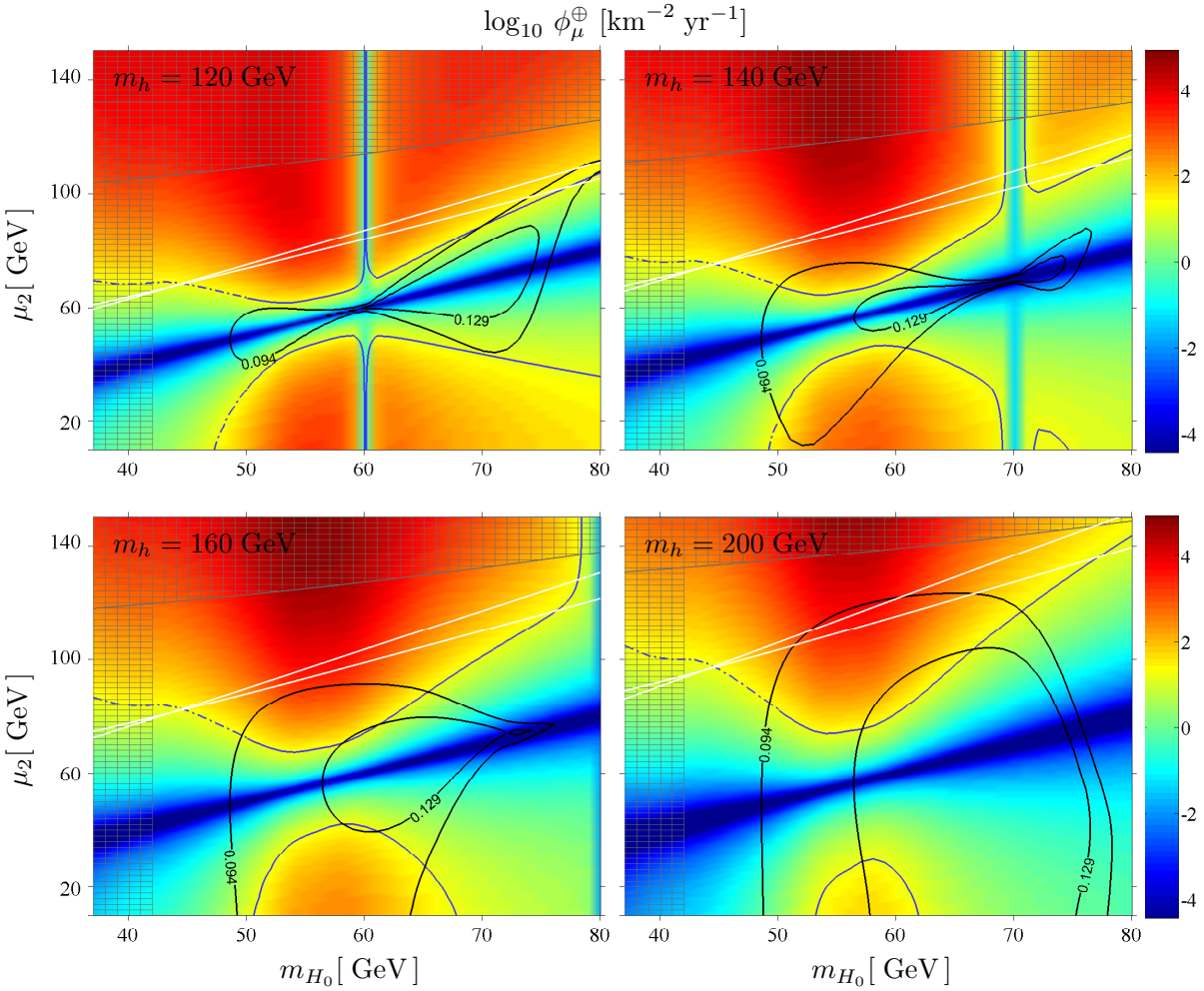

Figure 9: Muon flux resulting from mono-energetic neutrinos from the Earth for the IDM including light Majorana neutrinos.
Colour gradient - $\log_{10}\phi_\mu$ [km^{-2} yr^{-1}]*; WMAP area (black lines); XENON, CDMS exclusion limits (white lines); IceCube sensitivity hard (blue lines); excluded regions (shaded).*
(Parameters: $\lambda_2 = 0.2$, $\Delta m_{A_0 H_0} = 8\,GeV$, $\Delta m_{H^+ H_0} = 50\,GeV$, $m_N = 100\,GeV$, $h = 0.1$, $f = 0.3$*).*

6.3 High mass candidate: indirect detection from the Galactic centre

For the dark matter mass range under consideration in this section (500 GeV $\lesssim m_{H_0} \lesssim$ 1500 GeV),[7] the most promising signal of annihilation products comes from the Galactic centre. Earth and Sun can not produce large muon fluxes since the cross section of dark matter on nuclei, which is inversely proportional to the square of the mass of the candidate, is too small.

In the framework of the basic IDM and for this mass range, annihilation into pairs of W or Z gauge bosons, or into Higgs boson pairs, are dominant at tree level. Annihilation into fermion-antifermion pairs through a Higgs boson, especially into $t\bar{t}$, is also possible. However, for the parameter range considered here, these channels turn out to be negligible.

The Higgs boson and the gauge bosons give distinct neutrino spectra. Those originating from

[7]Higher masses are in principle possible, but the range given here is conservative, in the sense that we do not considered large quartic couplings [11].

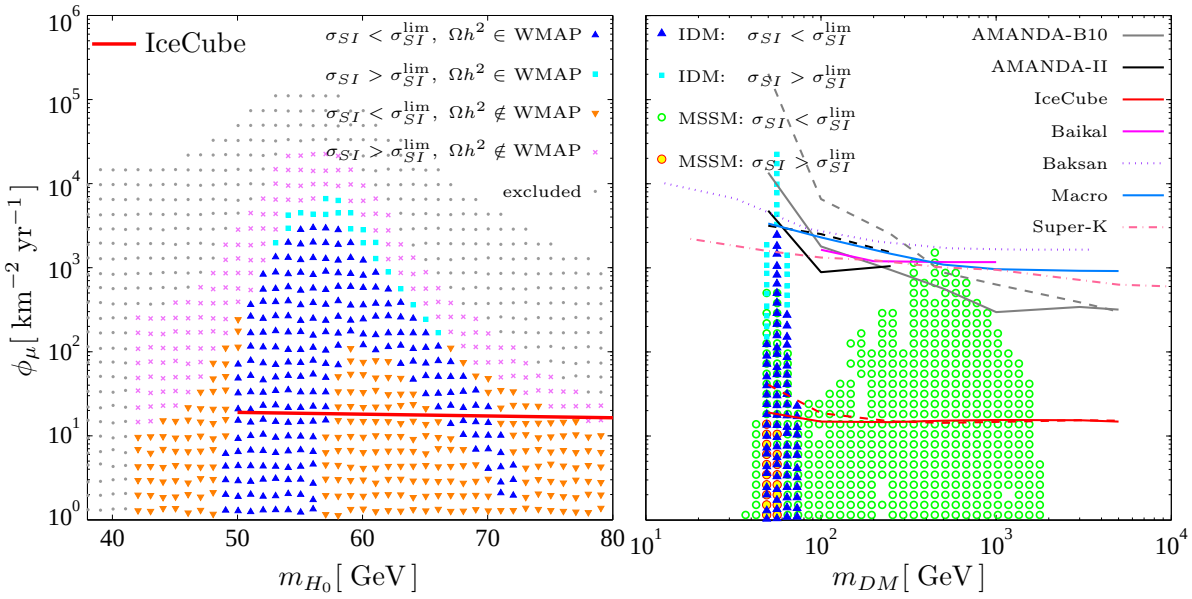

Figure 10: Scattered Plots of the muon fluxes of IDM and MSSM from the Earth. IDM fluxes result from mono-energetic neutrinos from the addition of light Majorana neutrinos.
left: The blue points (upward triangles) correspond to combinations of parameters that are in agreement with 2σ WMAP and direct detection limits, the light blue ones (squares) are in agreement with 2σ WMAP but the cross section is above the direct detection limit, the orange ones (downward triangles) are outside the 2σ WMAP region but the cross section is in agreement with direct detection, the magenta ones (crosses) violate both constraints. The grey points (dots) are excluded by other constraints (e.g. vacuum stability). The red line gives the IceCube sensitivity for a hard neutrino spectrum.
right: All plotted points are within the 3σ WMAP region. The blue ones correspond to the IDM with Majorana extension (dark blue below, light blue above direct detection limit). The green and yellow points are predicted by the MSSM (yellow below, green above direct detection limit). The lines are different detector thresholds: AMANDA-B10 (1997-1999) hard (solid) and soft (dashed); AMANDA-II (2001-2003) hard (solid) and soft (dashed); IceCube best case hard (solid) and soft (dashed); BAIKAL (1998-2001); BAKSAN (1978-1995); MACRO (1989-1998) hard; SUPER-K (1996-2001) soft, see ref. [50] and references therein.
(Parameters: $m_h = 200\,GeV$, $\lambda_2 = 0.2$, $\Delta m_{A_0 H_0} = 8\,GeV$, $\Delta m_{H^+ H_0} = 50\,GeV$, $f = 0.3$, $m_N = 100\,GeV$, $h = 0.1$*).*

W and Z are considered as hard neutrinos: they have a flat spectrum and a significant fraction has high energies. Those produced through the decay of the Higgs are comparatively softer. The amount of hard neutrinos among the total neutrino flux is primarily determined by the branching ratio into W^+W^- and ZZ.

In ref. [11], it has been shown that, for the mass range 500 GeV $\lesssim m_{H_0} \lesssim$ 1500 GeV, the abundance is in agreement with WMAP for $m_{H_0} \sim \mu_2$. Furthermore, all but a thin band around the diagonal is excluded by vacuum stability and perturbativity. In the following, we consider μ_2 in the range $m_{H_0} - 20$ GeV $\lesssim \mu_2 \lesssim m_{H_0} + 15$ GeV and parameterize the m_{H_0}-μ_2 plane by $(m_{H_0};\, \mu_2 - m_{H_0})$. The diagonal in the $(m_{H_0};\, \mu_2)$ representation becomes the horizontal $\mu_2 - m_{H_0} = 0$. For the Higgs mass and the mass splittings, we follow the choice made in the same reference, $m_h = 120$ GeV,

$\Delta m_{A_0 H_0} = 5$ GeV and $\Delta m_{H^+ H_0} = 10$ GeV. The coupling $\lambda_2 = 0.2$ chosen as in the previous sections completes the parameters set.

The abundance, computed with micrOMEGAs, is shown in figure 11. The WMAP region is drawn in black, solid (dash-dottet) lines corresponding to the 2σ (resp. 3σ) range. The exclusion limits (shaded region), as well as the WMAP area, lie, as expected, close to the horizonal line, $\mu_2 - m_{H_0} = 0$. The limit from vacuum stability corresponding to $\lambda_2 = 0.2$ excludes the region $\mu_2 > m_{H_0}$. The exclusion limit below $\mu_2 = m_{H_0}$ results from the less strict perturbativity constraint, $1 < \lambda_i < 4\pi$.

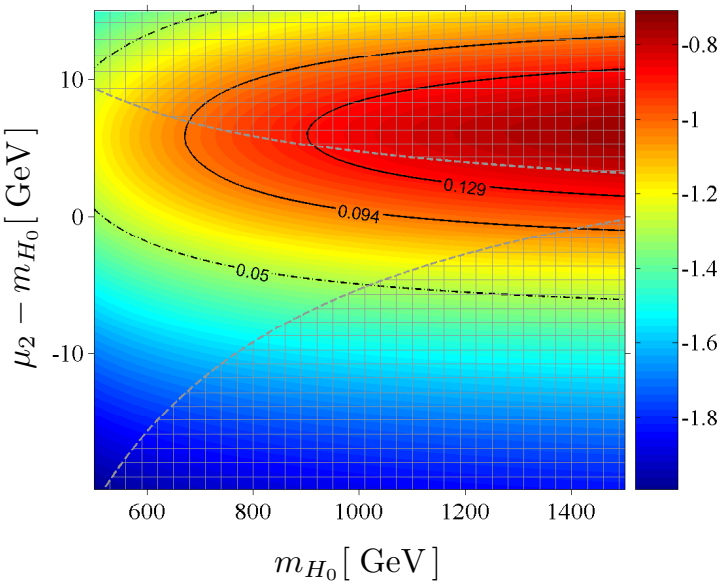

Figure 11: Dark matter abundance obtained from micrOMEGAs. The black lines represent the WMAP density range at 2σ (solid lines) and 3σ (dash-dotted line). The shaded regions are excluded by vacuum stability (upper part) and by perturbativity (lower part).
Colour gradient - $\log_{10} \Omega h^2$*; WMAP area (black lines); excluded regions (shaded).*
(Parameters: $m_h = 120\,GeV$, $\lambda_2 = 0.2$, $\Delta m_{A_0 H_0} = 5\,GeV$, $\Delta m_{H^+ H_0} = 10\,GeV$*).*

The cross sections for the different annihilation channels, the total annihilation cross section, and the branching ratios are also computed with micrOMEGAs for the given choice of parameters. It is found that, over the biggest part of the allowed region, the W^+W^- channel is dominant, followed by $Z\,Z$. The Higgs channel is only relevant in a region that is excluded by the constraints mentioned above, while $t\bar{t}$ is negligible everywhere. This implies that the neutrino flux is mainly hard for the mass range considered in this section.

The total flux of neutrinos from the Galactic centre is computed with eq. (22), for the chosen combinations of parameters. For this purpose, the integrated spectrum of neutrinos (*i.e.* the total number of neutrinos produced from all annihilation channels) is obtained from micrOMEGAs. This integration can be carried out for different energy thresholds. More precisely, we do not only compute the total number of muonic, but also that of electronic and tauonic neutrinos. Given the distance from the Galactic centre, after neutrino oscillations, the three generations arrive at the Earth with a ratio $\nu_\mu : \nu_\tau : \nu_e = 1 : 1 : 1$, and we obtain the flux of muon-neutrinos by averaging over all generations. In addition, we use the total annihilation cross section and $\overline{J}$ taken from section 5 for a NFW profile and the opening angle of the ANTARES detector, a neutrino telescope

that may look at the Galactic centre.

The resulting neutrino flux is shown in figure 12, assuming a detector threshold of 30 GeV, characteristic of that expected for ANTARES. In the plot on the left side, the colour gradient is representing $\log_{10}\phi_\nu$ [km^{-2} yr^{-1}] and the black lines correspond to the 2σ WMAP limit. The scattered plot on the right side gives the neutrino flux only for models that are not excluded by vacuum stability or perturbativity. The colour code corresponds to whether the abundance is in agreement with WMAP (dark blue) or not (light blue). The two red lines represent the sensitivity of the ANTARES detector found in ref. [56] for the two extremals of a purely hard (solid line) and a purely soft (dashed line) neutrino spectrum.

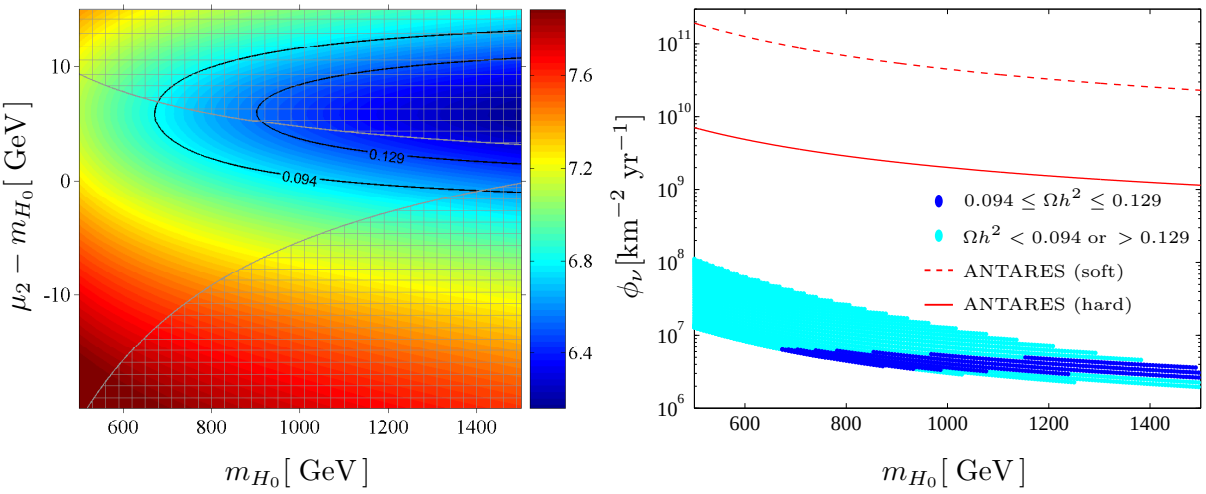

Figure 12: Expected neutrino flux in the ANTARES detector from the Galactic centre, for a NFW profile, and a threshold energy of 30 GeV.
left: The colour gradient represents $\log_{10}\phi_\nu$[km^{-2} yr^{-1}]. The WMAP region is drawn as black lines and the excluded areas are shaded.
right: Scattered plot of the neutrino flux together with the sensitivity of ANTARES for a soft (dashed) and a hard (solid) spectrum. The dark blue points lie within the WMAP area while the light blue ones are outside.
(Parameters: $m_h = 120\,GeV$, $\lambda_2 = 0.2$, $\Delta m_{A_0 H_0} = 5\,GeV$, $\Delta m_{H^+ H_0} = 10\,GeV$*).*

As in the non-excluded area, H_0 annihilates dominantly into W^+W^- and ZZ gauge bosons, with a branching ratio $\gtrsim 80\%$, the neutrino flux is mainly hard and has to be compared to the solid sensitivity curve. However, the expected neutrino flux lies between two and three orders of magnitude below the expected sensitivity of ANTARES.

As is usual in this discussions of indirect detection from the Galactic centre, we make use of the fact that the dark matter density profile in the innermost region of the Galaxy is poorly known and might be steeper than the assumed NFW profile and enhanced by some boost factor. For instance, in [12], the predicted gamma flux is boosted by a factor $\sim 10^4$ reflecting those uncertainties. The boost may also be partly of particle physics origin. The annihilation of heavy dark matter candidates that interact through relatively lighter particles (for instance, the W, the Z and the Higgs in the present case) may have a larger cross section for low relative velocities than that computed at tree level, a phenomenon called "Sommerfeld enhancement" [57, 58]. From the similarity of the IDM with Minimal Dark Matter models, the expected Sommerfeld enhancement in H_0 annihilations at the Galactic centre is $\mathcal{O}(10^2)$ at most but might be non-negligible. Regardless of the possibility

of boosting the flux, we must ensure that the signatures are not in contradiction with existing observations, say in gamma rays, see for instance ref. [59]. The observations of the EGRET satellite of the Galactic centre, which we take from the left-middle plot of figure 5c in ref. [60], set an upper limit on the gamma rays that may be produced in annihilations of the H_0. Similarly to the computation of the neutrino spectrum, we have used micrOMEGAs to obtain the differential photon spectrum, together with $\overline{J}$ for a NFW profile and an opening angle $\Delta\Omega = 10^{-3}$ corresponding to the resolution of EGRET (cf. section 5). For each point in the space of models, we may compute the gamma ray flux and compare it to EGRET data to derive a maximal boost factor (for the masses considered, the most constraining observations are at an energy $E_\gamma \approx 10$ GeV). Typically the maximal boost factors are $\sim 10^2 - 10^3$, which are actually quite moderate values, given the uncertainties on the Galactic abundance and the possibility of Sommerfeld enhancement. The maximum allowed neutrino flux is obtained according to

$$\phi_\nu^{\rm norm} \;=\; \phi_\nu^{\rm NFW}\,\frac{\phi_\gamma^{\rm EGRET}(E_{\rm norm})}{\phi_\gamma^{\rm NFW}(E_{\rm norm})}\,, \tag{27}$$

for each model. The result is shown in figure 13. In the left plot, the WMAP area is drawn in black and the excluded areas are shaded. The scattered plot on the right contains only points that are not excluded, together with the soft (given for information) and hard ANTARES sensitivities in red. As discussed above, the neutrino flux should be compared to the hard sensitivity (solid line), due to the large branching ratio into the W^+W^- and ZZ channels. The dark blue colour corresponds to models that agree within 2σ with WMAP, the light blue ones have too high or too low abundance.

For H_0 candidates with mass $\gtrsim 900$ GeV, the maximum muon flux is above the ANTARES sensitivity and several models have an abundance that is in agreement with WMAP. Similar predictions for the neutralino may be found in ref. [59].

7 Conclusion

In this paper, we have investigated the indirect detection signatures in neutrinos, for various scalar dark matter candidates within the framework of the Inert Doublet Model. Concretely, we have considered three distinct mass ranges. The first one corresponds to a rather light WIMP, $m_{H_0} \sim$ few GeV. This range is not excluded by existing direct detection experiments, and may be consistent with the combined results of DAMA/NaI and DAMA/Libra. We have shown that the neutrinos that are produced by a light H_0 captured in the Sun can be constrained by Super-Kamiokande measurements. This result corroborates the (model independent) statements made in refs. [18, 48]. We have also studied the predictions for more mundane WIMP candidates, corresponding to $m_{H_0} \sim 60$ GeV. Since the H_0 has only a SI cross section on nuclei, the best hope to detect its presence is in the Earth, in particular using the resonant scattering on iron. Such signatures have also been considered in [13] and our results for the fluxes are in agreement. However, direct detection strongly limits the potential of signatures from the Earth (see for instance ref. [61]), and the H_0 is no exception. In particular, we have found no solutions that give an observable signal from the Earth and are both in agreement with the WMAP abundance and direct detection exclusion limits. In order to boost the signal in neutrinos from the Earth, we have considered an extension with (light) Majorana neutrinos. The model has to be substantially fine-tuned to have WMAP abundance, capture in the Earth and strong annihilations into mono-energetic neutrinos (as well as reasonable SM neutrino masses), but some solutions may be possible. These are depicted in figure 10. Finally, we considered heavy WIMPs, $m_{H_0} \sim$ TeV. Those candidates annihilate at the centre of the Galaxy and produce high energy neutrinos that may be observable, provided a boost factor $\sim 10^3$.

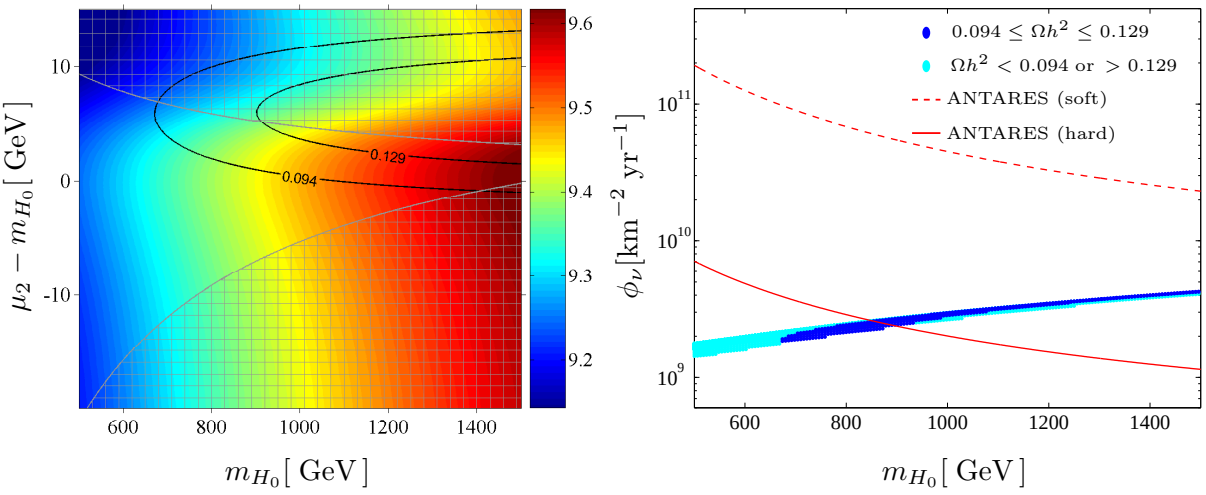

Figure 13: Upper limit on the expected neutrino flux from the IDM in the ANTARES detector. The neutrino flux of figure 12 is enhanced by a boostfactor factor in order to circumvent the astrophysical uncertainties on the dark matter profile at the Galactic centre and to obtain an upper limit on the expectable neutrino flux while leaving the corresponding γ-flux below the EGRET limit.
left: The colour gradient represents $\log_{10} \phi_\nu^{norm}$[km^{-2} yr^{-1}]. The WMAP region is drawn as black lines and the excluded areas are shaded.
right: Scattered plot of the neutrino flux together with the sensitivity of ANTARES for a soft (dashed) and a hard (solid) spectrum. The dark blue points lie within the WMAP area while the light blue ones are outside.
(Parameters: $m_h = 120\,GeV$, $\lambda_2 = 0.2$, $\Delta m_{A_0 H_0} = 5\,GeV$, $\Delta m_{H^+ H_0} = 10\,GeV$*).*

Note added in proof

Recent simulations of the dark matter halo in presence of a disk of baryons indicate that there might be a rotating disk of dark matter in our Galaxy [30]. Because of the small relative velocity between this so-called dark disk and the solar system, it has been shown in [62] that capture in the Earth, and to some extent in the Sun, might be dramatically enhanced. In that paper, the impact of the dark disk on the neutrino and muon fluxes from the Earth is illustrated for CMSSM neutralino candidates, but clearly similar enhancements should be expected for IDM dark matter candidates (*i.e.* in particular for a candidate close to the iron resonance, as considered in section 6.2). We keep for further work the investigation of this exciting possibility.

Acknowledgments

This work is supported by the FNRS and Belgian Federal Science Policy (IAP VI/11). The work of Q.S. and M.H.G.T is supported by the Belgian Fonds de la Recherche Scientifique (FNRS). One of us (S.A.) would like to thank Daan Hubert for discussions. We also thank Joakim Edsjö for help on using WimpSim and for enlightenment on capture in the Earth and Daniel Bertrand, Catherine De Clercq, Jean-Marie Frère and Emmanuel Nezri for discussions.

References

[1] U. Seljak, A. Slosar, and P. McDonald, "Cosmological parameters from combining the Lyman-alpha forest with CMB, galaxy clustering and SN constraints," *JCAP* **0610** (2006) 014, arXiv:astro-ph/0604335.

[2] **Particle Data Group** Collaboration, W. M. Yao *et al.*, "Review of particle physics," *J. Phys.* **G33** (2006) 1–1232.

[3] G. Jungman, M. Kamionkowski, and K. Griest, "Supersymmetric dark matter," *Phys. Rept.* **267** (1996) 195–373, arXiv:hep-ph/9506380.

[4] G. Bertone, D. Hooper, and J. Silk, "Particle Dark Matter: Evidence, Candidates and Constraints," *Phys. Rept.* **405** (2005) 279–390, arXiv:hep-ph/0404175.

[5] D. Hooper and S. Profumo, "Dark matter and collider phenomenology of universal extra dimensions," *Phys. Rept.* **453** (2007) 29–115, arXiv:hep-ph/0701197.

[6] N. G. Deshpande and E. Ma, "Pattern of Symmetry Breaking with Two Higgs Doublets," *Phys. Rev.* **D18** (1978) 2574.

[7] S. L. Dubovsky, P. G. Tinyakov, and I. I. Tkachev, "Massive graviton as a testable cold dark matter candidate," *Phys. Rev. Lett.* **94** (2005) 181102, arXiv:hep-th/0411158.

[8] E. Ma, "Verifiable Radiative Seesaw Mechanism of Neutrino Mass and Dark Matter," *Phys. Rev.* **D73** (2006) 077301, arXiv:hep-ph/0601225.

[9] R. Barbieri, L. J. Hall, and V. S. Rychkov, "Improved Naturalness with a Heavy Higgs: An Alternative Road to LHC Physics," *Phys. Rev.* **D74** (2006) 015007, arXiv:hep-ph/0603188.

[10] T. Hambye and M. H. G. Tytgat, "Electroweak Symmetry Breaking induced by Dark Matter," *Phys. Lett.* **B659** (2008) 651–655, arXiv:0707.0633 [hep-ph].

[11] L. Lopez Honorez, E. Nezri, J. F. Oliver, and M. H. G. Tytgat, "The Inert Doublet Model: an Archetype for Dark Matter," *JCAP* **0702** (2007) 028, arXiv:hep-ph/0612275.

[12] M. Gustafsson, E. Lundstrom, L. Bergstrom, and J. Edsjo, "Significant Gamma Lines from Inert Higgs Dark Matter," *Phys. Rev. Lett.* **99** (2007) 041301, arXiv:astro-ph/0703512.

[13] P. Agrawal, E. M. Dolle, and C. A. Krenke, "Signals of Inert Doublet Dark Matter in Neutrino Telescopes," arXiv:0811.1798 [hep-ph].

[14] E. Nezri, M. H. G. Tytgat, and G. Vertongen, "Positrons and antiprotons from inert doublet model dark matter," arXiv:0901.2556 [hep-ph]. arXiv:0901.2556.

[15] D. Majumdar and A. Ghosal, "Dark Matter candidate in a Heavy Higgs Model - Direct Detection Rates," *Mod. Phys. Lett.* **A23** (2008) 2011–2022, arXiv:hep-ph/0607067.

[16] S. Andreas, T. Hambye, and M. H. G. Tytgat, "WIMP dark matter, Higgs exchange and DAMA," *JCAP* **0810** (2008) 034, arXiv:0808.0255 [hep-ph].

[17] M. Taoso, G. Bertone, and A. Masiero, "Dark Matter Candidates: A Ten-Point Test," *JCAP* **0803** (2008) 022, arXiv:0711.4996 [astro-ph].

[18] J. L. Feng, J. Kumar, and L. E. Strigari, "Explaining the DAMA Signal with WIMPless Dark Matter," *Phys. Lett.* **B670** (2008) 37–40, arXiv:0806.3746 [hep-ph].

[19] C. Savage, G. Gelmini, P. Gondolo, and K. Freese, "Compatibility of DAMA/LIBRA dark matter detection with other searches," arXiv:0808.3607 [astro-ph].

[20] J. L. Feng, J. Kumar, J. Learned, and L. E. Strigari, "Testing the Dark Matter Interpretation of the DAMA/LIBRA Result with Super-Kamiokande," arXiv:0808.4151 [hep-ph].

[21] E. Lundstrom, M. Gustafsson, and J. Edsjo, "The Inert Doublet Model and LEP II Limits," arXiv:0810.3924 [hep-ph].

[22] Q.-H. Cao, E. Ma, and G. Rajasekaran, "Observing the Dark Scalar Doublet and its Impact on the Standard-Model Higgs Boson at Colliders," *Phys. Rev.* **D76** (2007) 095011, arXiv:0708.2939 [hep-ph].

[23] M. Cirelli, N. Fornengo, and A. Strumia, "Minimal dark matter," *Nucl. Phys.* **B753** (2006) 178–194, arXiv:hep-ph/0512090.

[24] R. A. Flores and J. R. Primack, "Observational and theoretical constraints on singular dark matter halos," *Astrophys. J.* **427** (1994) L1–4, arXiv:astro-ph/9402004.

[25] A. V. Kravtsov, A. A. Klypin, J. S. Bullock, and J. R. Primack, "The Cores of Dark Matter Dominated Galaxies: theory vs. observations," *Astrophys. J.* **502** (1998) 48, arXiv:astro-ph/9708176.

[26] J. F. Navarro, C. S. Frenk, and S. D. M. White, "The Structure of Cold Dark Matter Halos," *Astrophys. J.* **462** (1996) 563–575, arXiv:astro-ph/9508025.

[27] B. Moore *et al.*, "Dark matter substructure within galactic halos," *Astrophys. J.* **524** (1999) L19–L22.

[28] J. Diemand *et al.*, "Clumps and streams in the local dark matter distribution," arXiv:0805.1244 [astro-ph].

[29] V. Springel *et al.*, "The Aquarius Project: the subhalos of galactic halos," arXiv:0809.0898 [astro-ph].

[30] J. I. Read, G. Lake, O. Agertz, and V. P. Debattista, "Thin, thick and dark discs in LCDM," arXiv:0803.2714 [astro-ph].

[31] T. Bruch, J. Read, L. Baudis, and G. Lake, "Detecting the Milky Way's Dark Disk," arXiv:0804.2896 [astro-ph].

[32] M. W. Goodman and E. Witten, "Detectability of certain dark-matter candidates," *Phys. Rev.* **D31** (1985) 3059.

[33] W. H. Press and D. N. Spergel, "Capture by the sun of a galactic population of weakly interacting, massive particles," *Astrophys. J.* **296** (1985) 679–684.

[34] A. Gould, "Direct and indirect capture of WIMPs by the Earth," *Astrophys. J.* **328** (1988) 919–939.

[35] A. Gould and S. M. Khairul Alam, "Can heavy WIMPs be captured by the earth?," *Astrophys. J.* **549** (2001) 72–75, arXiv:astro-ph/9911288.

[36] T. Damour and L. M. Krauss, "A new solar system dark matter population of weakly interacting massive particles," *Phys. Rev. Lett.* **81** (1998) 5726–5729, arXiv:astro-ph/9806165.

[37] J. Lundberg and J. Edsjo, "WIMP diffusion in the solar system including solar depletion and its effect on earth capture rates," *Phys. Rev.* **D69** (2004) 123505, arXiv:astro-ph/0401113.

[38] A. H. G. Peter, "Dark matter in the solar system I: The distribution function of WIMPs at the Earth from solar capture," arXiv:0902.1344 [astro-ph.HE].

[39] A. H. G. Peter, "Dark matter in the solar system III: The distribution function of WIMPs at the Earth from gravitational capture," arXiv:0902.1348 [astro-ph.HE].

[40] P. Gondolo *et al.*, "DarkSUSY: Computing supersymmetric dark matter properties numerically," *JCAP* **0407** (2004) 008, arXiv:astro-ph/0406204.

[41] A. Gould, "Resonant enhancements in weakly interacting massive particle capture by the earth," *The Astrophysical Journal* **321** (Oct., 1987) 571–585.

[42] F. Halzen and D. Hooper, "Prospects For Detecting Dark Matter With Neutrino Telescopes In Light Of Recent Results From Direct Detection Experiments," *Physical Review D* **73** (2006) 123507, arXiv:hep-ph/0510048.

[43] P. Ullio, L. Bergstrom, J. Edsjo, and C. G. Lacey, "Cosmological dark matter annihilations into gamma-rays: A closer look," *Phys. Rev.* **D66** (2002) 123502, arXiv:astro-ph/0207125.

[44] M. Cirelli, R. Franceschini, and A. Strumia, "Minimal Dark Matter predictions for galactic positrons, anti-protons, photons," *Nucl. Phys.* **B800** (2008) 204–220, arXiv:0802.3378 [hep-ph].

[45] J. Edsjö, "WimpSim Neutrino Monte Carlo.". http://www.physto.se/∼edsjo/wimpsim/.

[46] M. Blennow, J. Edsjo, and T. Ohlsson, "Neutrinos from WIMP Annihilations Using a Full Three- Flavor Monte Carlo," *JCAP* **0801** (2008) 021, arXiv:0709.3898 [hep-ph].

[47] G. Belanger, F. Boudjema, A. Pukhov, and A. Semenov, "micrOMEGAs2.0: A program to calculate the relic density of dark matter in a generic model," *Comput. Phys. Commun.* **176** (2007) 367–382, arXiv:hep-ph/0607059.

[48] D. Hooper, F. Petriello, K. M. Zurek, and M. Kamionkowski, "The New DAMA Dark-Matter Window and Energetic-Neutrino Searches," arXiv:0808.2464 [hep-ph].

[49] **Super-Kamiokande** Collaboration, S. Desai *et al.*, "Search for dark matter WIMPs using upward through-going muons in Super-Kamiokande," *Phys. Rev.* **D70** (2004) 083523, arXiv:hep-ex/0404025.

[50] **IceCube** Collaboration, D. Hubert and A. Davour, "Search for neutralino dark matter with the AMANDA neutrino telescope," in *30th International Cosmic Ray Conference (ICRC 2007)*. 2007.

[51] F. Petriello and K. M. Zurek, "DAMA and WIMP dark matter," *JHEP* **09** (2008) 047, arXiv:0806.3989 [hep-ph].

[52] CDMS-Collaboration, "A Search for WIMPs with the First Five-Tower Data from CDMS," arXiv:0802.3530 [astro-ph].

[53] J. Kubo, E. Ma, and D. Suematsu, "Cold dark matter, radiative neutrino mass, mu $\rightarrow$ e gamma, and neutrinoless double beta decay," *Phys. Lett.* **B642** (2006) 18–23, arXiv:hep-ph/0604114.

[54] **Particle Data Group** Collaboration, C. Amsler *et al.*, "Review of particle physics," *Phys. Lett.* **B667** (2008) 1.

[55] C. Arina and N. Fornengo, "Sneutrino cold dark matter, a new analysis: relic abundance and detection rates," *JHEP* **11** (2007) 029, arXiv:0709.4477 [hep-ph].

[56] D. J. Bailey, *Monte Carlo tools and analysis methods for understanding the ANTARES experiment and predicting its sensitivity to Dark Matter*. PhD thesis, Wolfson College, Oxford, 2002.

[57] J. Hisano, S. Matsumoto, M. M. Nojiri, and O. Saito, "Non-Perturbative Effect on Dark Matter Annihilation and Gamma Ray Signature from Galactic Center," *Phys. Rev.* **D71** (2005) 063528, arXiv:hep-ph/0412403.

[58] M. Cirelli, A. Strumia, and M. Tamburini, "Cosmology and Astrophysics of Minimal Dark Matter," *Nucl. Phys.* **B787** (2007) 152–175, arXiv:0706.4071 [hep-ph].

[59] G. Bertone, E. Nezri, J. Orloff, and J. Silk, "Neutrinos from Dark Matter annihilations at the Galactic Centre," *Physical Review D* **70** (2004) 063503. http://arxiv.org/abs/astro-ph/0403322.

[60] S. D. Hunter *et al.*, "EGRET Observations of the diffuse Gamma-Ray Emission from the Galactic Plane," *The Astrophysical Journal* **481** (May, 1997) 205–240.

[61] V. D. Barger, W.-Y. Keung, and G. Shaughnessy, "Monochromatic Neutrino Signals from Dark Matter Annihilation," *Phys. Lett.* **B664** (2008) 190, arXiv:0709.3301 [astro-ph].

[62] T. Bruch, A. H. G. Peter, J. Read, L. Baudis, and G. Lake, "Dark Matter Disc Enhanced Neutrino Fluxes from the Sun and Earth," arXiv:0902.4001 [astro-ph.HE].